



BRAINsens: Body-Worn Reconfigurable Architecture of Integrated Network Sensors

Ruhi Mahajan¹ · Bashir I. Morshed² · Gavin M. Bidelman³

Received: 6 May 2018 / Accepted: 20 August 2018
© Springer Science+Business Media, LLC, part of Springer Nature 2018

Abstract

Body sensor network (BSN) is a promising human-centric technology to monitor neurophysiological data. We propose a fully-reconfigurable architecture that addresses the major challenges of a heterogenous BSN, such as scalability, modularity and flexibility in deployment. Existing BSNs especially with Electroencephalogram (EEG) have these limitations mainly due to the use of driven-right-leg (DRL) circuit. We address these limitations by custom-designing DRL-less EEG smart sensing nodes (SSN) for modular and spatially distributed systems. Each single-channel EEG SSN with an input-referred noise of $0.82 \mu V_{\text{rms}}$ and CMRR of 70 dB (at 60 Hz), samples brain signals at 512 sps. SSNs in the network can be configured at the time of deployment and can process information locally to significantly reduce data payload of the network. A Control Command Node (CCN) initializes, synchronizes, periodically scans for the available SSNs in the network, aggregates their data and sends it wirelessly to a paired device at a baud rate of 115.2 kbps. At the given settings of the I²C bus speed of 100 kbps, CCN can configure up to 39 EEG SSNs in a lego-like platform. The temporal and frequency-domain performance of the designed “DRL-less” EEG SSNs is evaluated against a research-grade Neuroscan and consumer-grade Emotiv EPOC EEG. The results show that the proposed network system with wearable EEG can be deployed in situ for continuous brain signal recording in real-life scenarios. The proposed system can also seamlessly incorporate other physiological SSNs for ECG, HRV, temperature etc. along with EEG within the same topology.

Keywords Body sensor network · Driven-right-leg circuit · Fully reconfigurable architecture · I²C bus · Wearable EEG

Introduction

Body Sensor Networks (BSN) with wearable physiological sensors can provide quality of care for those who need frequent and yet unobtrusive health monitoring. There are several wearable health monitoring systems developed in the recent years to provide low-cost, continuous all-day and any-place physiological monitoring, eg., CodeBlue [1],

Mercury [2], SATIRE [3], GumPack [4] and few other in the literature [5–7]. Some other BSN, for instance, LiveNet [8], AMON [9], LifeGuard [10] and reconfigurable wireless nodes [11, 12] are also developed for vital data monitoring (Electrocardiography (ECG), Blood Pressure), activity tracking and galvanic skin response (GSR) measurement.

For BSNs with EEG, several studies have featured wireless EEG monitoring using commercial-off-the-shelf (COTS) components and custom-fabricating ICs [13–15]. A portable 8-channel EEG has been described in [16] which uses long lead wires to sense the signals and connects to the main module for wireless data streaming using ZigBee. Human++ [17], CleveMed [18], MICA2 [19, 20], QUASAR’s sensing technology [21] are also reported in the literature. To the best of our knowledge, all of the above-mentioned research-prototypes as well as commercial EEG systems like Emotiv [22], Muse [23], Neurosky [24], etc. have a rigid architecture in terms of their number of channels. None of the existing wireless EEG devices is reconfigurable, intelligent, modular and scalable. They are designed for a fixed number of channels.

This article is part of the Topical Collection on *Mobile & Wireless Health*

✉ Ruhi Mahajan
er.ruhimahajan@gmail.com

¹ Center for Biomedical Informatics, University of Tennessee Health Science Center, Memphis, TN, USA

² Department of Electrical and Computer Engineering, University of Memphis, Memphis, TN, USA

³ School of Communication Sciences & Disorders, University of Memphis, Memphis, TN, USA

However, a similar study of EEG sensing with scalable nodes is reported [25, 26] but, it is based on capacitive EEG sensing, which is noise prone and suffers from micro-motion of electrodes with respect to skin, compared to the traditional impedimetric contact-based EEG sensing approach.

In this study, we propose BRAINsens (body-worn reconfigurable architecture of integrated network sensors) – a reconfigurable architecture for BSN where any sensor node can communicate in a modular fashion to the central node, leading to a lego-like paradigm which can be customized at the time of deployment. Among other physiological sensors, modularization of the EEG and ECG is more challenging because these low voltage signals are easily contaminated by the common-mode and power-line interference. So, we limit the scope of this study to investigate and implement EEG modularization. Compared to the aforementioned BSNs, the proposed BRAINsens has following unique features:

- 1) *EEG modularization*: Elimination of DRL circuit from the conventional EEG system by designing a novel analog front end, which thereby provides modularization in EEG sensing.
- 2) *Reconfigurability*: All the sensors in the network are hardware-reconfigurable and Lego-like connectable which offers ease of deployment.
- 3) *Scalability*: Hardware design for neurophysiological sensors can be easily upgraded without the redesign of entire system network because each sensing node is independent. The network can include physiological sensors like ECG, pulse oximeter, temperature, orientation sensors, etc. along with the EEG in the same topology.
- 4) *Distributed intelligence*: The sensing nodes address the challenge of the data payload in the integrated sensing network by incorporating distributed intelligence.

The following sections give details on the overall system architecture, hardware design, fabrication of EEG nodes, and communication protocol of the network. The results for the EEG system validation and comparison with other commercial EEGs are also discussed.

Overall system design

BRAINsens offers a sensor-centric approach with Smart sensing nodes (SSN) built with instrumentation hardware that can process data locally before sending it to the Command control node (CCN). The system is fully-adaptive irrespective of the type of SSN (EEG, ECG, temperature, etc.) in the network. All SSNs are connected with the CCN via a shared high-speed digital Inter-Integrated Circuit (I²C) bus [27]. The envisioned BRAINsens is reconfigurable at all abstraction levels, which includes deployment, BSN, and sensor level.

The main reason of non-modularity of sensors in existing EEG is due to the use of driven-right-leg (DRL) circuit in the hardware design. The DRL circuit helps reduce common-mode interference. But, it is designed on the basis of a fixed number of channels to be used in the system. Thus, it does not allow scalability at the time of deployment. In this study, however, we propose a novel analog front end (AFE) design for EEG which will not need DRL and thus sensor level modularization can be implemented.

Hardware design of EEG SSN

The hardware for the EEG SSN is designed to sense very low-voltage brain signals (10–200 microvolt range) from the scalp. Each EEG SSN has a single-channel, referential montage based AFE with a very low-noise INA-118 instrumentation amplifier (Texas Instruments, TX, USA) at the first stage of the signal conditioning circuit. This instrumentation amplifier (inst-amp) offers a very high input impedance ($10^{10} \Omega$ typical) to the two input channels, referred as Ch1 and reference, and amplifies the difference between these inputs with a gain of 26. In contrast, using DRL to reduce power-line interference in the circuit, we have employed a unity gain Twin-T active notch filter ($f_c = 60$ Hz) at the second stage. The noise suppression at the early stage of instrumentation circuit improves the noise figure of the overall circuit. We further limit the bandwidth of the circuit between $f_c = 0.16$ –47.5 Hz with the designed active band-pass filters that provide an overall mid-band gain of 55.2 dB. For more details on this “DRL-less” AFE design, please refer to our previous studies in [28, 29]. For ECG sensing, a similar SSN node design can be used after modifying the gain and filter bandwidth.

The supply voltage, V_{dd} (3.3 V) and the ground of the SSN node are routed through the CCN using a 6-pin ribbon cable (discussed in a later section). The analog signal is referenced to the mid-rail voltage (1.65 V) by creating a virtual ground supply on the node that consists of a voltage-divider followed by a unity gain buffer. We used AD8607 (Analog Devices Inc., MA, USA), a dual-channel rail-to-rail input and output, an operational amplifier in the AFE design because of its low noise (22 nV/ $\sqrt{\text{Hz}}$), very low input bias current (1pA max) and micro power consumption (50 μA max.).

The analog brain signals are digitized on the SSN node using an ultra-low power 16-bit MSP430F5528 microcontroller (Texas Instruments, TX, USA) with its in-built 12-bit successive approximation register (SAR) ADC at 512 sps. Once triggered by the CCN, SSN continuously samples the signals and saves the results in a 1 KB buffer. The sampled data is sent upon request to the CCN through a digital I²C bus at the speed of 100 kbps.

Hardware design of CCN

CCN has a TI MSP430F5659 microcontroller unit (MCU) connected with its peripherals including Bluetooth module, LEDs, and I²C connectors. The 16-bit RISC architecture based MCU has 64 KB SRAM and 512 KB flash memory, sufficient to process multiple SSNs data. The CCN is connected with a 3.3 V Li-poly battery that can be charged on the board through a charge management controller via micro-USB cable.

We also used RN-42, a Class 2 wireless Bluetooth (BT) module (Roving Networks, CA) which has integrated folded PCB antenna for 2.4 GHz ISM band. This BT module (26 μA sleep, 3 mA connected, and 30 mA transmit) allows the UART communication in Serial Port Profile (SPP) mode. To reduce current consumption, MCU uses auxiliary system clock (ACLK) operating at 32.768 kHz for the timer (used for 1 s delay) and a high-frequency sub-main clock (SMCLK) at 1 MHz for the I²C and universal asynchronous receiver transmitter (UART) communication.

The CCN uses a 6-pin I²C connector dedicated to each SSN in the prototype. The 4 pins of this connector constitute I²C bus – V_{dd}, GND, Serial data (SDA) and Serial clock (SCL), 5th pin is for the reference channel (shared among the network for EEG/ECG sensing), whereas 6th pin is not used. Figure 1 shows the functional block diagram for both EEG SSN and CCN.

Hardware design of miscellaneous nodes

In order to keep the body potential within the acceptable range of the AFE, a virtual ground potential (V_{gnd} = 1.65 V) is separately generated and applied through a V_{gnd} node. The circuit consists of a voltage divider followed by the high input impedance buffer designed with an AD8607 operational amplifier. The V_{gnd} potential is fed to the body by placing the V_{gnd} node on the mastoid of the subject for EEG sensing. For ECG and other physiological sensing, the location of V_{gnd} node can be changed to the right leg. To implement the referential montage of EEG, an independent node is designed to sense the

reference channel signal. This node does not have any analog or digital circuit components instead, it has only an electrode connector that can be snapped to an EEG/ECG electrode. This sensed reference signal is communicated to other SSN nodes of the network through the I²C bus using reference channel wire within the I²C bus. For EEG sensing, the reference node is attached on the mastoid of the subject.

We have designed 4-layer (top, V_{dd}, GND, bottom) printed circuit boards (PCB) for all prototype nodes using Allegro PCB designer (Cadence Design Systems, Inc., CA, USA), fabricated it through a commercial PCB foundry (OSH Park, OR, USA), and manually populated them in our lab. Figures 2 and 3 represent the fully assembled EEG SSN, CCN, reference and V_{gnd} nodes of the BRAINSens system.

I²C communication protocol

To ensure connectivity of the sensors in a Lego-like fashion, we have used I²C protocol that allows a user to connect multiple SSNs on the same shared digital bus. Each SSN connected to the bus is software addressable by a unique address and connected to the bus with its SDA and SCL pulled up with 4.7 kΩ resistors. We have used 7-bit addressing mode at a standard bus speed of 100 kbps, according to which the minimum value of pull-up resistor, R_p (min) to be used is computed as:

$$R_{p(\min)} = \frac{V_{dd} - 0.4V}{3mA} = \frac{3.3 - 0.4V}{3mA} = 9.66.6\Omega \tag{1}$$

According to the I²C bus specifications, the maximum bus capacitance, C_b should not exceed from 400 pF. The measured bus capacitance on SDA and SCL (including trace lengths) is found to be ~10 pF, which indicates that we can practically connect up to 39 SSNs in the network with the given design. However, more SSNs can be included in the architecture by using shorter cable length (to keep C_b < 10 pF) or by using bus buffers and switched pull-up circuits in the design that can cope with excess bus capacitance [27]. In comparison with the Serial Peripheral Interface (SPI) communication, I²C allows us to add

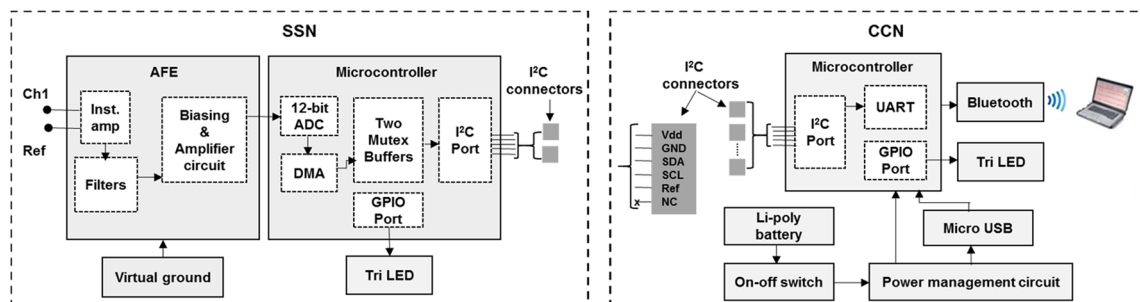
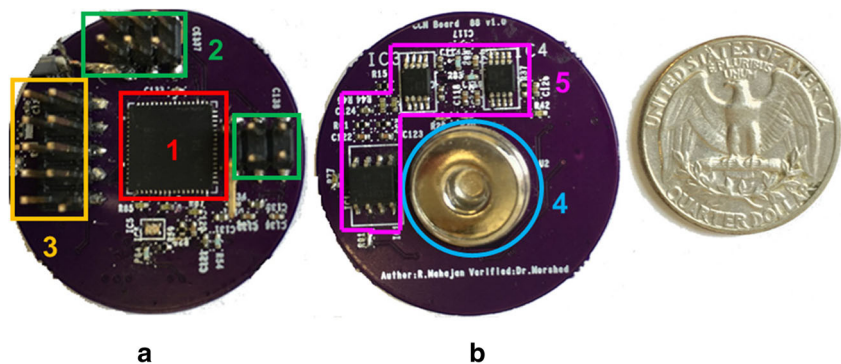


Fig. 1 The functional block diagram of different nodes of BRAINSens (Left) EEG SSN and (Right) CCN. The hardware for all the nodes is made up of surface mount commercial off-the-shelf (COTS) components.

I²C bus is shared between various nodes of BRAINSens via a 6-pin connector on each node

Fig. 2 Photograph of a fully assembled EEG SSN (diameter 1.29") for the BRAINsens system. **a** Top view of the hardware. **b** Bottom view of the hardware beside a quarter coin. Legends: (1) MCU (2) I²C connectors (3) Spy-Bi-wire JTAG programming connector (4) EEG electrode connector (5) AFE



multiple SSNs in the system without the need of additional select line, thereby providing hardware modularity in the proposed system design while keeping the number of wire requirement to a minimum [30–32].

Reconfigurable software firmware

The firmware of the MCU for SSN and CCN are developed with a TI Code Composer Studio (CCS) and programmed to the MCU with a Spy-Bi-wire JTAG programmer through in-circuit serial programming port. The CCN and SSN are employed in the single master-multislave configuration of I²C topology in the network. Each SSN is identified by its unique pre-defined address as per the 7-bit I²C addressing protocol. In this study, the starting address of the SSN is 71 (0x41h).

The SSN is the slave of the system that is driven by the SCL generated by the CCN. On the power reset, SSN remains in the idle mode unless it receives a “general call” command on the I²C bus, in response to which the SSN starts sampling the signals. An in-built ADC12 of MCU is used for sampling (see Rx ISR of Fig. 4). The ADC12 uses a sampling timer mode to trigger the sampling every 1.9 ms (desired for EEG sensing). In order to reduce the average current-consumption and increase the throughput of I²C module, a Direct Memory Access

(DMA) controller is used to move the ADC12 conversion results to one of the available Mutex-buffers (each of size 1 KB). Initially, the DMA controller saves the conversion results in buffer 1, if this buffer is full then it saves in buffer 2 and vice-versa by checking the flags inside the DMA interrupt service routine (ISR). To avoid the buffer overflow in the network, the time required in filling the buffer, T_{buffer} (~973 ms) follows the following constraint:

$$T_{buffer} = \frac{T_{smp} \times S_{buffer}}{S_{ADC}} \geq T_{trans} \quad (2)$$

where T_{trans} is the time required to transmit each buffer data (~82 ms by the I²C bus), T_{smp} is the sampling time, S_{buffer} is the size of the buffer and S_{ADC} is the size of digitized ADC data (number of samples) in bytes.

In this study with three prototype EEG SSNs, data is requested by the CCN every 1 s that guarantees the time constraint mentioned in eq. 2. For every data request, SSN executes the Transmission ISR (see Tx ISR in Fig. 4) according to which if any of the buffers is full, then 1 KB is transmitted over the I²C bus, otherwise, SSN sends 0x33h (arbitrarily selected number) to indicate that none of the buffer is full and I²C bus is released.

The CCN is the only master of the system and thus initiates the network communication by generating SCL. On the

Fig. 3 Photograph of fully assembled **a** CCN (1.96 × 1.33“), **b** Virtual ground node (diameter: 0.95”) and (c) Reference node (diameter: 0.91”). Legends: (1) MCU (2) Charge management controller (3) Micro-USB port (4) I²C connectors (5) Voltage divider circuit for V_{gnd} (6) Electrode connector

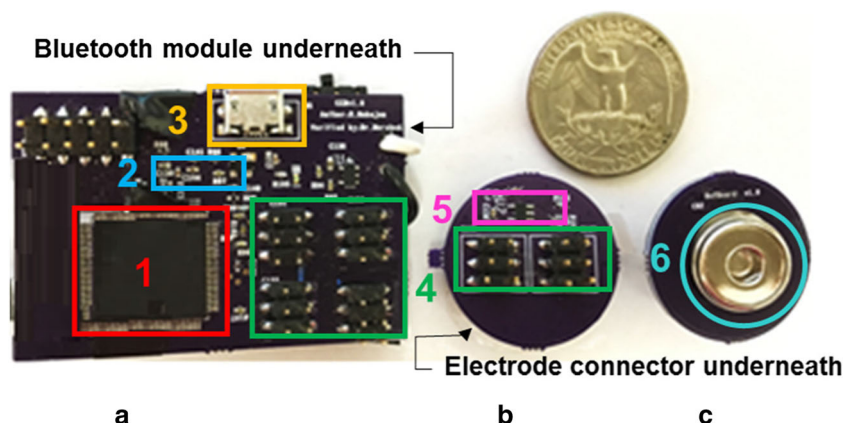
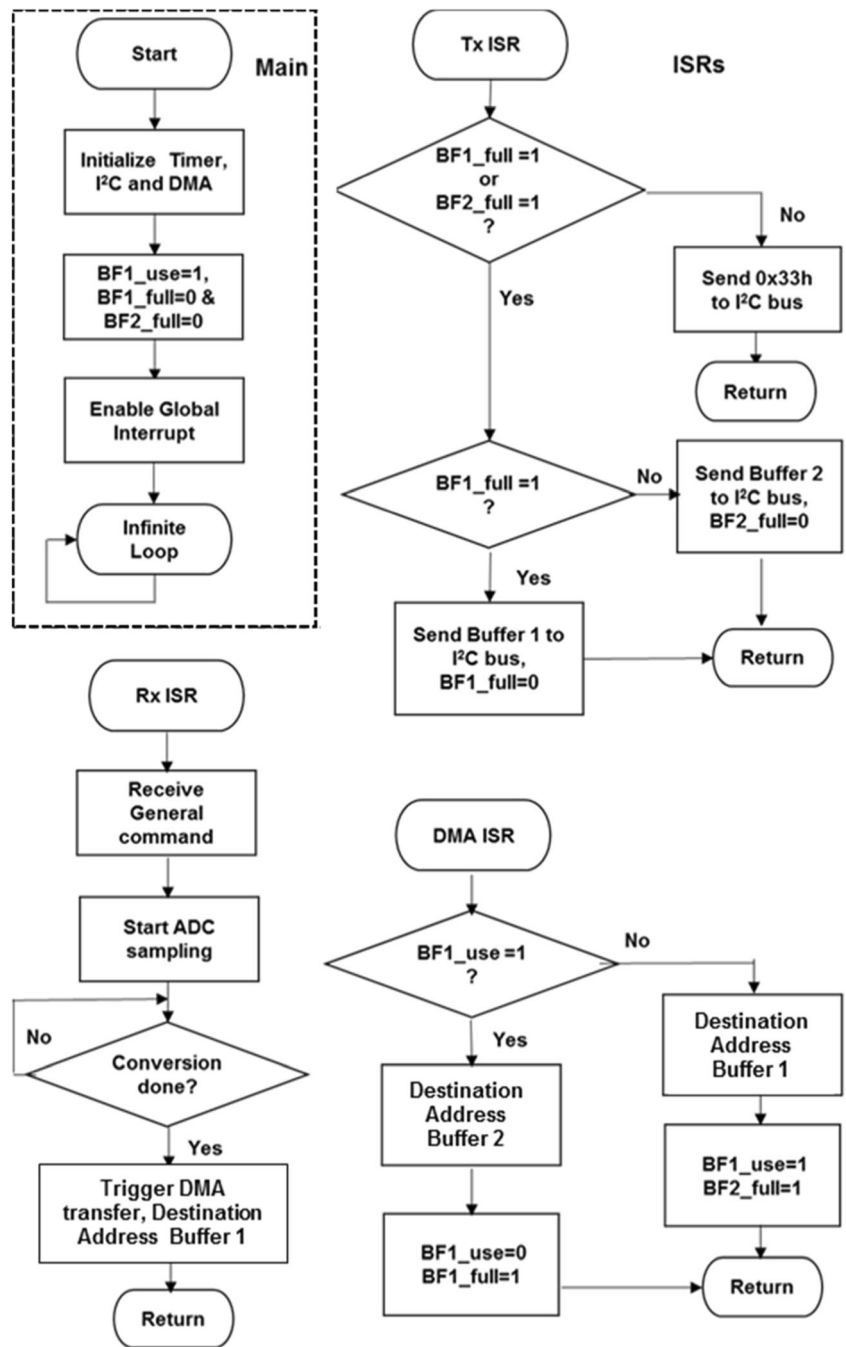


Fig. 4 Flowchart for the SSN firmware with the main routine and interrupt service routines for DMA controller, I²C transmission, and I²C receive communication with the CCN

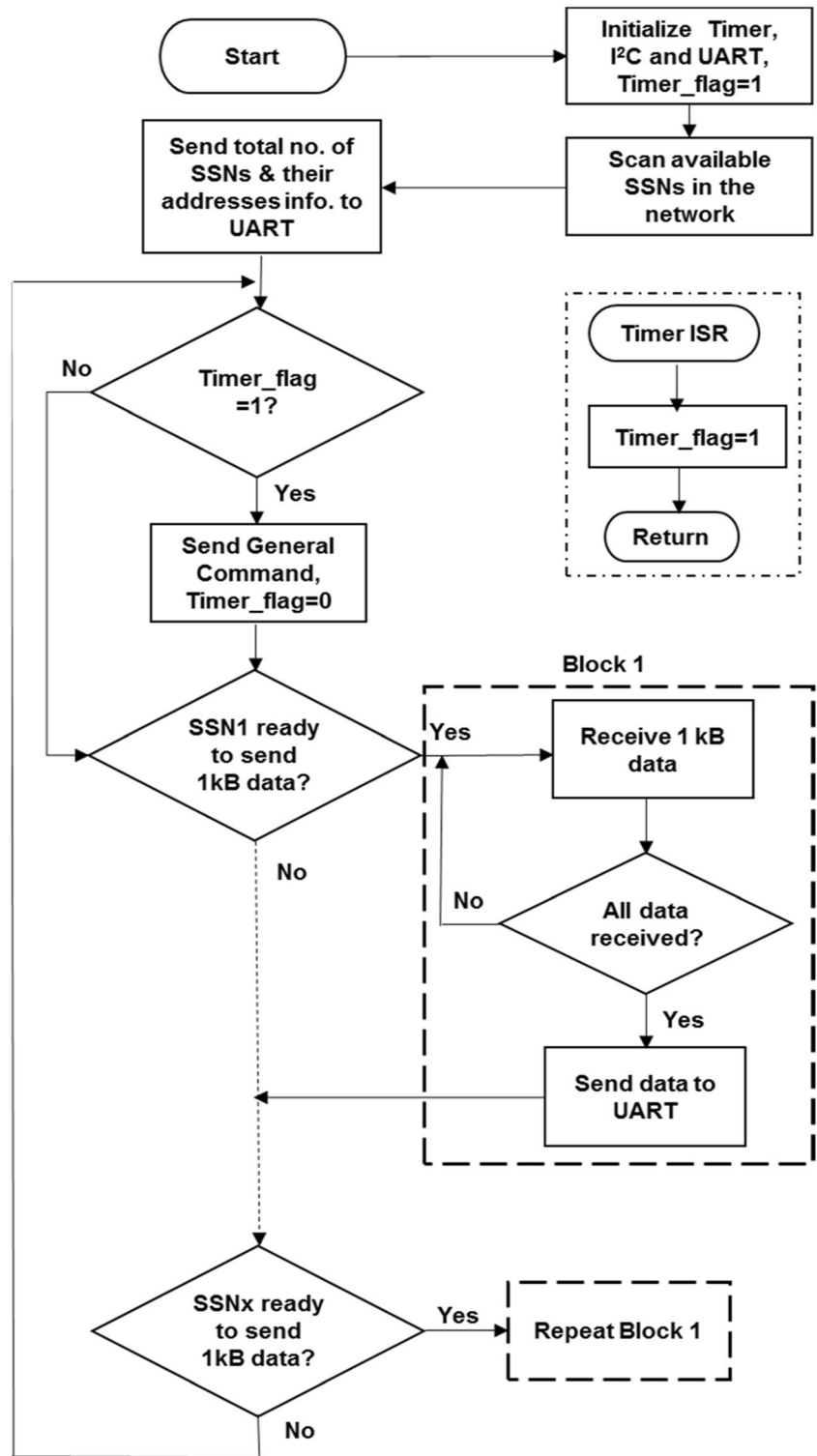


power reset, CCN identifies the total number of SSNs available in the network along with their corresponding addresses and sends this information to the Bluetooth module through UART at 115.2 kbps baud rate. The CCN then issues a “general call” command (0x55h, arbitrary selected) simultaneously to all the available SSNs to trigger sampling of the signals. The MCU of the CCN uses a 16-bit timer for 1 s (can be modified) to trigger the general call periodically so as to keep all the SSNs synchronized. The CCN further aggregates data from the available SSNs in a round-robin

topology and sends data to the UART for wireless transmission to a paired laptop/PC.

CCN sends 1025 bytes of data to the UART, the first byte represents the SSN ID followed by 1024 bytes of the SSN data. Figure 5 represents the flowchart of the reconfigurable CCN firmware. The reconfiguration ability of the CCN allows it to dynamically allocate memory to save the SSN data if any new SSN is found in the network. In order to avoid data loss, the sampling time for the sensors should satisfy the constraint:

Fig. 5 Flowchart for the CCN firmware depicting its data communication protocol with multiple SSNs in a round-robin topology. A “general call” command to synchronize all the SSNs of the network is sent every 1 s



$$T_{\text{samp}} \geq \sum_N T_{\text{frame}} \tag{3}$$

where N is the number of homogeneous sensors and $T_{\text{frame}} = (T_{\text{clkbus}} * x)$; x is number of bits in the data packet and T_{clkbus} is the clock period for I²C bus.

Methods for system evaluation

The designed system with reconfiguration capability of EEG SSNs and CCN has been functionally verified both in the laboratory and naturalistic settings. This section describes methods used to evaluate the time-frequency response, noise

characteristics, power consumption of the nodes and signal processing techniques for comparison with commercial EEG systems.

Bench test experiments

The schematic of the AFE was simulated with OrCAD Capture CIS (Cadence Design Systems, CA, USA) simulation software for various amplitude and frequency ranges of the input sine-wave signal.

Fidelity measurement

Fidelity reflects the stability of the gain in a specific bandwidth. The fidelity characteristics of the circuit were recorded in the simulation and were then compared with the actual measurements. For the measurement, the input channel, Ch1 of one of the EEG SSN was connected to a sine input signal ($V_{in} = 3 \text{ mV}_{p-p}$, at different frequencies between 1 to 100 Hz) from a 2-channel signal generator (DG4062, RIGOL Tech., Beijing, China). The output measurements were recorded using a digital storage oscilloscope (DSO-X 2024 A, Agilent Tech., CA, USA) with respect to the V_{gnd} .

Linearity measurement

The linearity characteristic of the circuit represents the stability of the gain with respect to different input voltages. Simulation results from the Cadence were saved in the *.csv file and later plotted in the MATLAB against the actual measurement. To generate microvolt range signals (for direct comparison with EEG signals), a 20 dB attenuator was used at the output of the RIGOL signal generator.

Common-mode rejection analysis

In order to investigate the common-mode rejection ratio (CMRR) at 60 dB, common mode gain (A_{cm}) and differential mode gain (A_{dm}) were calculated. To measure the common-mode signal, the reference channel and Ch1 channel of the inst-amp were tied together and were driven with a 100 mV_{p-p} sine signal at 60 Hz from the signal generator. However, A_{dm} at 60 Hz was measured by applying a differential mode sine input, $V_{dm} = 3 \text{ mV}_{p-p}$ between Ch1 and Ref channels. CMRR of the circuit was then mathematically calculated as:

$$\text{CMRR} = 20 \log_{10} \frac{A_{dm}}{A_{cm}} \text{dB} \quad (4)$$

All output measurements recorded with the oscilloscope were with respect to the V_{gnd} .

Power management and consumption

BRAINsens uses a Li-Poly battery (3.3 V, 800 mAh) as the power supply. The battery was connected with the CCN and can be charged using a 5-pin micro-USB cable through an on-board linear charge management controller (MCP73831, Microchip Tech., AZ, USA) that avoids over-charging of the battery. The power supply to the SSN and other peripheral nodes in the network was supplied using the 6-pin ribbon cable. The hardware components were carefully selected to reduce the power consumption of the BRAINsens. The average current consumption was measured with the functional I^2C and UART communication.

In-vitro experiments

Data acquisition with EEG SSN

EEG SSNs along with the other peripherals were deployed on the subjects in real-life settings for continuous data collection. In this study, we attached the V_{gnd} and Ref nodes to the left and right mastoid of the subject, respectively. However, these locations for a different study can be changed without any constraint. Pre-gelled adhesive disposable sensors (GS26, Biomedical Instruments) were used with SSNs, which were snapped to one side of the SSN. To decrease the skin impedance before data collection, the skin of the subjects was gently abraded with Nuprep gel (DO Weaver & Co., CO, USA). Once the SSNs and other nodes were deployed, data was collected in real-time by CCN via I^2C protocol and sent to its serial port. The serial port was then read through the designed Graphical User Interface (GUI) in the MATLAB (MathWorks, MA, USA) in the paired laptop/ PC. This GUI also checks if any packet is lost due to the Bluetooth communication and notifies the user by displaying “*Packet Missed*” on the command window in MATLAB.

Data acquisition with Neuroscan

Neuroscan, a commercially available EEG system with wall-powered, 64-channel SynAmps RT amplifiers (Compumedics Neuroscan Ltd.) was used to compare the simultaneously recorded brain signals with our EEG SSNs. The RT amplifier has a low-noise 24-bit ADC, high CMRR of 110 dB and input impedance $>10 \text{ G}\Omega$ [33]. In this study, only two channels of the amplifier were used to compare with two EEG SSNs at AF3 and AF4 frontal lobe locations. Neuroscan uses Ag/AgCl disc electrodes (connected to the amplifier with 1 m cables). These electrodes were placed side-by-side ($<1 \text{ cm}$) to the GS26 electrodes on the frontal and mastoid sites. The data was recorded from two subjects for multiple sessions in a magnetically shielded room for $\sim 50 \text{ s}$ at $f_s = 500 \text{ sps}$. The electrode impedance was maintained $<5 \text{ k}\Omega$ throughout the

Table 1 BRAINsens's Specifications with EEG SSN

Parameter	Notes
Differential Amp.	Gain = 26
Low-pass filter	2rd order Butterworth, $f_c = 47.5$ Hz, Gain = 1.61
High-pass filter	Passive filter at $f_c = 0.1$ Hz, Gain = 0.83
Notch filter	Twin-T filter at $f_c = 60$ Hz, $Q = 0.1$, Gain = 1
Biasing Amp.	Non-inverting amplifier, Gain = 17.5
Range (input referred)	5500 $\mu\text{Vp-p}$
Coupling mode	DC coupled
Voltage Resolution	0.80 mV (1 LSB, input referred)
Digital Input	12-bit
Input-referred noise	0.82 μVrms
Fidelity	54.95 dB
Linearity	55.20 dB
CMRR	70 dB at 60 Hz
Signal to Noise ratio	126 dB
Supply voltage	3.3 V provided by CCN
Weight	6.43 g (SSN) [Other nodes- 11.94 g (CCN), 3.48 g (Ref) and 3.72 g (V_{gnd})]
Input Impedance	1010 Ω (typical for the differential mode)
Communication range	10 m

session. During the data collection, subjects did not perform any specific cognitive task rather they sat on a chair in the relaxed position. However, they were asked to blink when instructed (every five seconds).

Data acquisition with Emotiv EPOC

Another 14-channel commercial EEG device, EPOC (Emotiv, Eveleigh, NSW, Australia) was used to compare the brain activities [22]. EPOC was considered for the comparison because its specifications- such as battery-operation, referential montage based, wireless, low-cost EEG are very similar to the EEG SSN. EPOC has inbuilt analog filters with bandwidth 0.2–45 Hz, digital notch filters at $f_c = 60$ Hz to eliminate the power-line interference and 16-bit ADC to sample data at 128

sps. EPOC headset uses wet electrodes soaked in a saline solution. As the bulky EPOC headset occupies most of space on the scalp, only one EEG SSN was deployed on the subject at AF4 location. The data acquisition was conducted in an office environment in the naturalistic settings for ~ 100 s.

Data pre-processing and analysis

For one-to-one comparison between systems, signals were pre-processed to keep the same bandwidth and sampling rate. For example, Neuroscan signals were up-sampled at 512 sps and digitally filtered at 0.16–47 Hz using the Curry 7 Neuroimaging suite (Compumedics USA, Inc., NC, USA), whereas, EEG SSN signals were down sampled to 128 sps for the comparison with EPOC. Signals from both devices

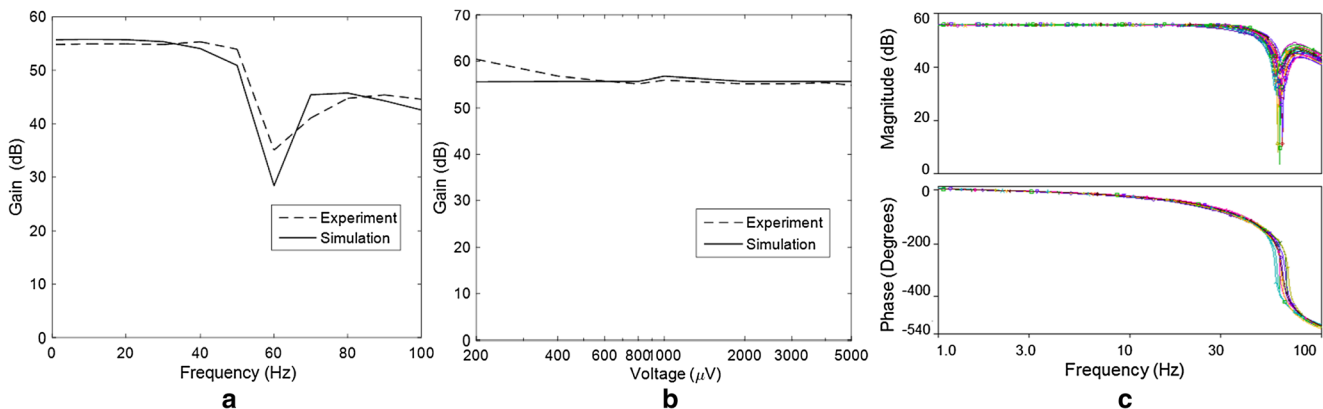


Fig. 6 Experiment and OrCAD simulation characteristic results for one of the EEG SSN **a** Fidelity and **b** Linearity, x-axis is in log scale. **c** Worst-case magnitude and phase response obtained with Monte Carlo simulation analysis

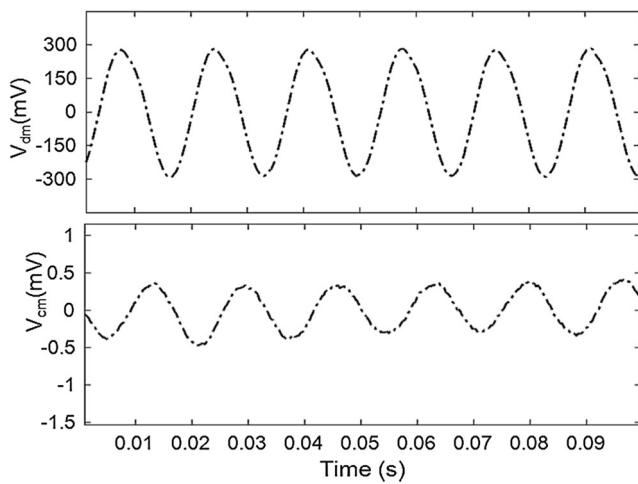


Fig. 7 CMRR measurement for an EEG SSN at 60 Hz (Top) Differential-mode response to a representative 3 mV_{p-p} test sine input applied between Ch1 and Ref channels of inst-amp. (Bottom) Common-mode response to a 100 mV_{p-p} test sine input applied to Ch1 (with Ch1 and Ref channels shorted)

were further digitally low-pass filtered from 1 to 40 Hz and notch filtered at 60 Hz in MATLAB.

To compare the systems, we computed wavelet coherence (WCO) between the signals to measure correlations in the time-frequency plane. WCO was computed with the *wcoher* function in MATLAB as:

$$WCO = \frac{|S(P_x^*(a, b)P_y(a, b))|^2}{S(|P_x(a, b)|^2)S(|P_y(a, b)|^2)} \quad (5)$$

where, $P_x(a, b)$ and $P_y(a, b)$ are the continuous wavelet transforms of signals x and y at scale a & position b , S is the smoothing operator in time & scale and superscript $*$ is the complex conjugate.

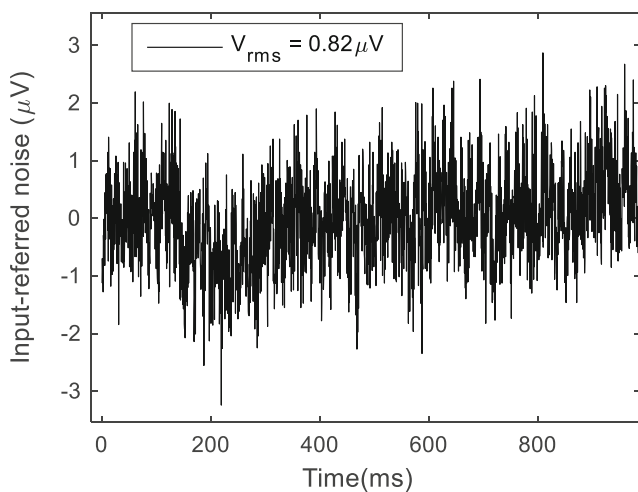


Fig. 8 Measured EEG SSN input-referred noise. The output noise is divided by the total gain of the system

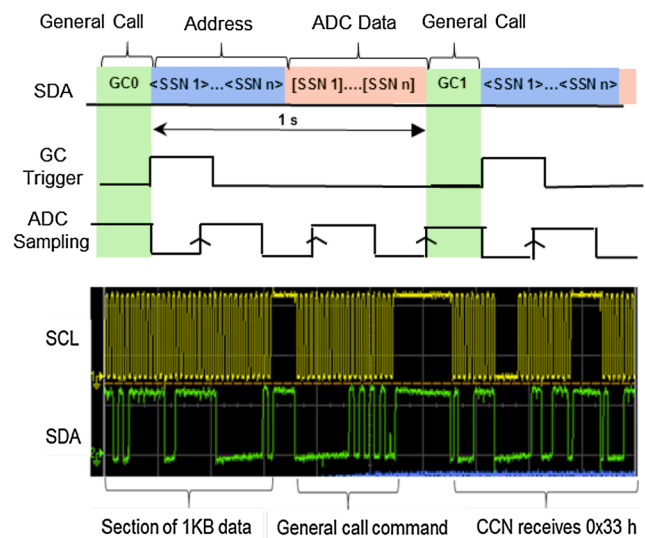


Fig. 9 (Top) Implemented I²C protocol. (Below) Snapshot of the actual SCL and SDA signals of the I²C bus as measured with the oscilloscope. The “general call” (GC) data 0x55h sent at address 0x00h along with SSN’s ADC data can be observed. The addition or removal of SSN in the network will reflect bit changes in SDA and SCL

Results

The time- and frequency-domain responses to the input signals for all EEG SSNs were functionally verified. Some of the observed technical specifications for the EEG SSN are tabulated in the Table 1. This study includes the results of only one randomly selected EEG SSN because the results were similar for the other SSNs. Figure 6 compares the experimental linearity and fidelity characteristics of the SSN. As observed in the Fig. 6a, there is a sharp attenuation at 60 Hz, which is due to the notch filter in the circuit. The measured average fidelity in the linear range was found to be ~54.95 dB. Whereas, the average measured linearity is observed to be 55.20 dB. The experimental values are slightly less than the theoretical simulation values, mainly because of the component tolerances and parasitic capacitances on the PCB. Also, in Fig. 6b, at the lower input voltages up to 400 μV, the measured linearity differs from the simulated curve, which might be due to the noise level of the oscilloscope. A Monte-Carlo analysis of the schematic was

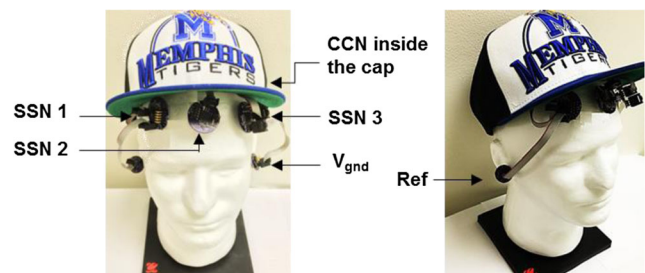


Fig. 10 Photograph of three prototype EEG SSN nodes deployed on a mannequin head. CCN is concealed inside the cap

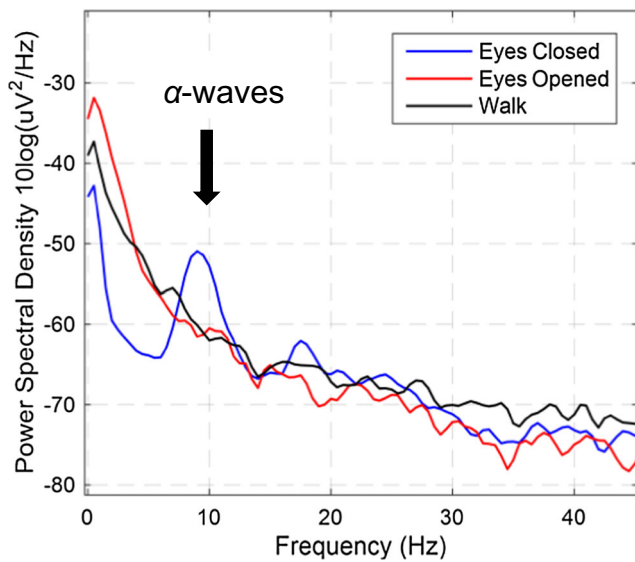


Fig. 11 The power spectral density of a 50 s continuous recording session from a male subject from AF3 location. The subject was instructed to keep his eyes closed, followed by eyes open and then to walk in the lab-settings

also performed with Cadence by using the actual tolerances of resistors and capacitors. Figure 6c shows the worst-case magnitude and phase response of the circuit for 50 runs.

As noted previously, the AFE of the EEG SSN does not have a DRL circuit, which is used in conventional EEG systems to reduce common-mode interference. Instead, we employed a high CMRR inst-amp followed by an active notch filter in the early stage of instrumentation circuit that mitigates the effect common-mode and power-line interference. To investigate the CMRR of the circuit specifically at 60 Hz, A_{dm} and A_{cm} were calculated at 60 Hz. The differential-mode output, V_{dm} is ~ 570 mV_{p-p} for 3 mV_{p-p} input signal as shown in the Fig. 7 (top) which yields $A_{dm} = 190$. Similarly, A_{cm} is found to be close to 0.06 for the common-mode output, $V_{cm} = 0.6$ mV_{p-p}. Further, using Eq. 4, the effective CMRR was found to be 70 dB. This CMRR should be good enough to suppress the power-line interference during the data acquisition. The DC bias was removed from the common-mode and

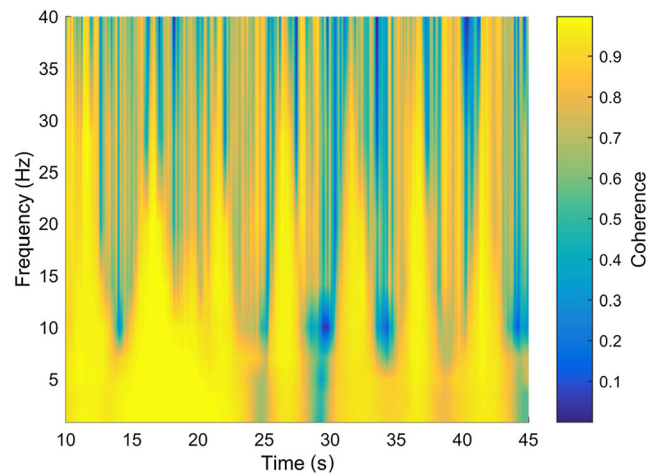


Fig. 13 Wavelet coherence measured between the signals of Neuroscan and BRAINsens EEG for the same data range as in Fig. 14. WCO is normalized between 0 to 1

differential-mode output signals of the circuit for clarity in Fig. 7. The noise in the EEG SSN was also measured with the oscilloscope, with both Ch1 input and Ref channel tied to the mid-rail. The recorded output noise waveform was divided by the system gain (575.43) so as to generate an input-referred noise waveform. The root-mean-square (RMS) measure, V_{rms} of the recorded input-referred-noise was plotted in MATLAB as shown in Fig. 8.

The I²C protocol of the network was also verified with bench tests. The measured rise time and fall time of the SDA and SCL was less than the maximum acceptable limits of 1000 ns and 300 ns respectively, as per the I²C specifications [27]. Figure 9 depicts a section of the 1 KB data transfer between the SSN and CCN as measured with the oscilloscope. The section also represents the “general call” command of data 0x55h sent at a 0x00h address for all the SSNs in the network to start ADC sampling. This is followed by 0x33h data from the SSN address 0x47h (71) indicating that the buffer of the SSN was not yet full to send the data. Empirical observations indicated that most of the power in the BRAINsens was consumed by the Bluetooth module

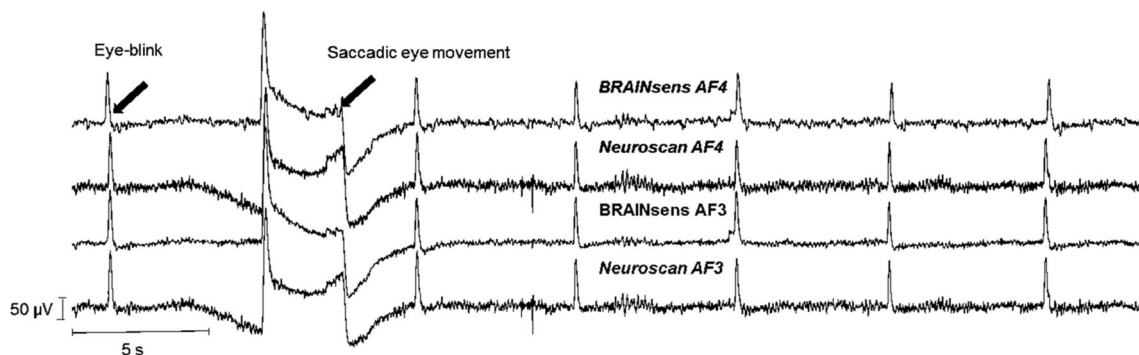


Fig. 12 EEG signals recorded from the AF3 and AF4 locations from Neuroscan and BRAINsens’s EEG SSN from a subject for around 35 s. Seven eye-blinks after every 5 s can be noticed. A rapid eye-movement by the subject can also be observed across all signals

(3 mA connected and 30 mA in the transmit mode). The ultra-low power TI microcontroller on the nodes was considered to consume up to 295 μ A in the active mode at 1 MHz. The average-current consumption was measured from the CCN and other peripherals by measuring the voltage drop (in the oscilloscope) across the 1.2 Ω resistor in series with the battery. CCN consumed an average current of 3.41 mA when connected with no SSN, 5.83 mA when connected with 1 SSN and 11.6 mA with 2 SSNs connected. Thus, with 2 SSNs, EEG data can be continuously recorded up to 69 h. (~ 3 days).

Further, the bench-tested EEG SSNs were used to measure actual EEG signals from the frontal lobe location of two subjects. Figure 10 shows the way the network EEG SSN nodes are deployed on the subjects. One of the recordings from a male subject was conducted for 50 s with initial 20 s with his eyes closed, next 15 s with natural eye-movements and last 15 s while walking. The power spectral density (PSD) for 10 s duration for each activity is plotted in Fig. 11. Typical alpha-waves (10 Hz) were observed during the eyes closed condition. Also, power spectrum during walk session was relatively higher for frequencies above 28 Hz compared with other two sessions, likely due to the frontalis and temporal muscle activity as mentioned in [34].

Furthermore, EEG SSNs were compared against commercial systems. Figure 12 represents a representative time segment (arbitrarily chosen) from the SSN of BRAINsens and Neuroscan system. Eye-blinks are evident after every ~5 s as per the protocol. The signal patterns of the EEG SSN, as well as sensitivity to the eye-blinks, were found to be very similar to the Neuroscan for both subjects and channels. For quantitative comparison, wavelet coherence was computed for both channels as shown in Fig. 13. The plot shows high correlation of around 0.9 between the signals especially in delta (1–4 Hz), theta (4–7 Hz), alpha (8–13 Hz) and beta (14–20 Hz) bands. These EEG bands are important to understanding EEG dynamics during working memory, attention-related processing, and other BCI applications [35]. Correlations were lower (~0.7) in the high beta (20–30 Hz) band, which may be due to different analog filtering specifications of these devices.

The time-domain Emotiv signals against BRAINsens signal from a subject at the AF4 location are also plotted in Fig. 14. Similar to the Neuroscan system, BRAINsens is comparable to the known standard, Emotiv. To compare the power

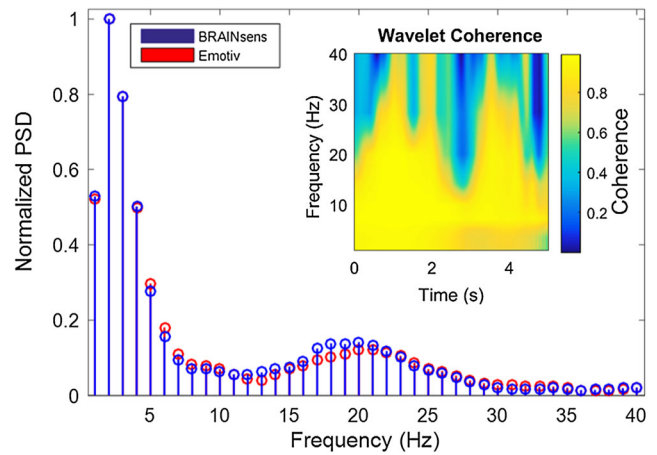


Fig. 15 Normalized stem plot for the PSD of BRAINsens's EEG SSN and Emotiv EPOC's recorded data from AF4 location. Measured WCO is embedded in the plot depicting the strong correlation between the signals

of the two signals at different frequencies, a min-max normalized PSD estimate was computed using Welch's method (with hamming window of length 512 over FFT length of 1024) in MATLAB. Figure 15 shows the corresponding PSD stem plots indicating a good correlation between the signals for most of the frequencies.

Discussion

The structure of the BRAINsens allows the user to deploy SSNs on any location of the body, in comparison to most of the existing devices with fixed location of channels. The envisioned BRAINsens would have modular EEG and other physiological sensors in the same I^2C topology. We limit the scope of this paper for the design and implementation of EEG modularization. However, a similar study based on monitoring heart rate variability (HRV) along with EEG has been conducted in our pilot studies [36]. Furthermore, our other studies have examined the implementation of hardware-efficient signal processing algorithms like ocular artifact removal [37], seizure prediction [38], feature extraction, etc. that can be implemented on the EEG SSNs and other SSNs which would be useful for many real-time BCI and classification applications.

The existing systems allow full-configurability on the sensor-hardware and BSN level as mentioned in Section "Introduction".

Fig. 14 A section of the simultaneously recorded EEG signals from Emotiv and BRAINsens for 16 s from AF4 location. Eye-blinks and other ocular artifacts can be noted

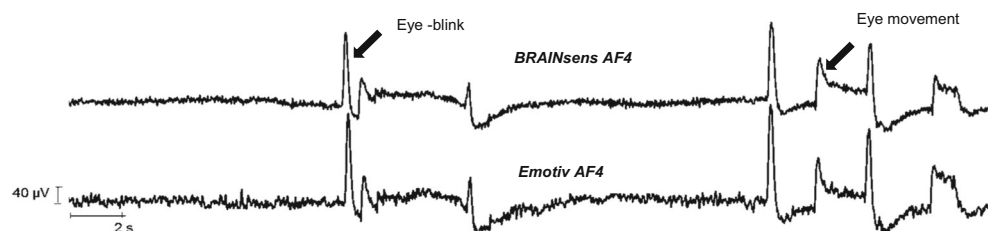


Table 2 Comparison with the commercial and research use EEG

Specifications	Neuroscan [30]	EPOC [22]	Muse [23]	MICA-2 [19]	CleveMed [40]	Human++ [17]	QUASAR [21]	This work
ADC resolution (bit)	24	1616	10 10	10	10 up to 16	10 12	16 16	10 12
Sampling Rate (Hz)	up to 20 K	128	220/500	200	up to 960	1024	1200	512
Bandwidth (Hz)	DC-3500	0.2-45	60 Hz notch	40	0.5-250	Unknown	50	0.16-47.5
DRL/CMS	Yes	Yes	Yes	No	Unknown	Unknown	Yes	No
No. of channels	up to 70	14	4	6	8	up to 24	10	up to 39
Reconfigurable	No	No	No	No	No	No	No	Yes
Battery life	Wall-powered	12 h.	5 h.	5 h.	8 h.	Unknown	72 h.*	46 h. **
Connectivity	Wired	Prop. wireless 2.4 GHz	Bluetooth 2.1 + EDR	ZigBee Radio transceiver	RF 2.4-2.48 GHz ISM	Radio Transceiver 2.4 GHz	Ethernet/Bluetooth	Bluetooth 2.6 GHz

* With 2 AAA batteries, other devices use compact Li-poly batteries

**When 3 SSNs are connected with an 800 mAh battery

But, the envisioned BRAINsens would allow reconfiguration on the deployment level as well so that the user can configure the sampling rate, ADC resolution, channel selection, etc. from a PDA. This parameter configuration would be crucial for the networks with high-density EEG to avoid network congestion and cope with data payload requirements.

The power consumption of the wearable BSN is one of the major concerns especially when battery-powered sensors are used. In this study, we have used carefully selected components with low power consumption. At present, system consumes ~20 mW per SSN when connected with a 3.3 V Li-poly battery of 800 mAh. Therefore, a fully charged battery would allow continuous data collection up to six days with one EEG SSN. The power of the designed system will be further optimized in the future work by using the sniff mode of the Bluetooth, ultra-low power modes of the microcontroller unit (e.g., LPM3/ LPM4) and dynamic frequency scaling techniques [39].

Table 2 compares some of the features of the designed system with other similar systems reported in the literature. This study is the first to report sensor-level reconfigurability for impedimetric EEG sensing. Most of the existing systems use DRL and focus on designing a BSN with a dedicated number of channels. Modular and easily deployable EEG systems are critically important especially for patients with neurological disorders (Alzheimer, Autism Spectrum Disorder, Post-Traumatic Stress Disorder, and Attention Deficit Hyperactivity Disorder), elderly vitality monitoring and emergency care conditions. The proposed technology in this paper supports very low-cost patient-centric healthcare, and will demonstrate effectiveness and usability of a healthcare monitoring in natural environments.

Conclusion

We have demonstrated the design of a hardware reconfigurable smart EEG sensing node (SSN) for a scalable architecture, BRAINsens, a wearable body sensor network (BSN). The proposed hardware resolves modularity in EEG and ECG systems, which is challenging mainly because of use of the DRL circuit. To address this concern, we have implemented a novel analog front-end design of the SSN, which achieves an input-referred noise of 0.82 μV_{rms} , and CMRR up to 70 dB (at 60 Hz) without using DRL. The elimination of DRL allows flexibility to the user to connect multiple EEG sensing nodes in a modular fashion. The designed single-channel EEG SSNs capture brain signals at a sampling rate of 512 sps and transmit them to a control node using a digital I²C bus. For future applications, SSNs are equipped with microcontrollers to process the local information to combat the challenges of data payload requirement. The control node (CCN) of the network scans for the available SSNs in the network, allocates memory for them and

aggregates their data, which is then sent to a paired device via Bluetooth at 115.2 kbps baud rate. The CCN dynamically adapts to the change in system configuration (e.g., number of attached SSNs) without hardware re-design. At the I²C bus speed of 100 kbps, up to 39 EEG SSNs can be connected to the network with each SSN consuming around 5 mA current, allowing continuous data collection for ~5 days by a 3 EEG SSN system with a 800 mAh Li-poly battery without recharging. The prototypes were functionally validated against two commercial EEG systems and the results suggest that the proposed system design can be deployed for comparable neurological data collection in real-life-settings. This research paves the path for a fully reconfigurable architecture of integrated network sensors that can seamlessly incorporate any types of heterogeneous body-worn sensor nodes (wired or wireless, temperature, pulse oximeter, ECG, etc.) along with the EEG within the same network.

Funding This work was partially supported by FedEx Institute of Technology Innovation Grant, The University of Memphis, TN, USA under Grant Number: 2013–537908.

Compliance with ethical standards

Conflicts of interest All authors declare that they have no conflict of interest.

Ethical approval This study involves the human participation and hence was pre-approved by the University of Memphis Institutional Review Board committee (Approval Number: 2289). The system's safety, deployment, acquisition protocol and recruitment process were evaluated by the committee.

Informed consent Informed consent was obtained from all individual participants included in the study.

References

- Malan, D., *et al.*, Codeblue: An ad hoc sensor network infrastructure for emergency medical care. Int. Workshop on Wearable and Implantable Body Sensor Networks. 5, 2004.
- Lorincz, K. *et al.*, Mercury: a wearable sensor network platform for high-fidelity motion analysis. *Sens. Syst.* 9:183–196, 2009.
- Ganti, R. *et al.*, SATIRE: A Software Architecture for Smart Attire. In: 4th Int. conf. on Mobile systems, applications and services, pp. 110–123, June 2006.
- Kejia, L., and Warren, S., GumPack: A Personal Health Assistant with Reconfigurable Surface Components. *J. Healthcare Eng.* 4(1): 145–166, 2013.
- Choudhury, T., *et al.*, The mobile sensing platform: An embedded system for capturing and recognizing activities. *IEEE Pervasive Magazine*, 2008.
- R. DeVaul, *et al.*, MITHril 2003: applications and architecture. *IEEE Int. Symposium of Wearable Computing*, 4, 2003.
- Otto, C. A., Jovanov, E., and Milenkovic, A., "A WBAN-based system for health monitoring at home," 3rd IEEE EMBS Int. Summer School and Symposium on Medical Devices and Biosensors (ISSS-MDBS), pp. 20–23, 2006.
- Sung, M., Marci, C., and Pentland, A., Wearable feedback systems for rehabilitation. *J. Neuro Eng. Rehabilitation* 2:17, 2005.
- Anliker, U. *et al.*, AMON: A wearable multi parameter medical monitoring and alert system. *IEEE Trans. Inf. Technol. Biomed.* 8(4):415–427, Dec. 2004.
- Mundt, C. W. *et al.*, A multi parameter wearable physiological monitoring for space and terrestrial applications. *IEEE Trans. Inf. Technol. Biomed.* 9(3):382–391, Sep. 2005.
- Riley, D, and Younis, M., A modular and power-intelligent architecture for wireless sensor nodes. *IEEE Conf. on Local Computer Networks*. 304–307, 2012.
- Gama, O., *et al.*, Towards a reconfigurable wireless sensor network for biomedical applications. *Sensors Technologies and Applications*. 490–495, 2007.
- Mohseni, P., and Najafi, K., Wireless multichannel Biopotential recording using an integrated FM telemetry circuit. 26th IEEE EMBS Annual Int. Conf., San Francisco, CA, pp. 4083–4086, 2004.
- P. Mohseni and Najafi, K., A battery-powered 8-channel wireless FM IC for biopotential recording applications. In: *Dig. Tech. Papers 2005 IEEE Int. Solid- State Circuits Conf.*, San Francisco, CA, pp. 560–561. 2005.
- Obeid, I., Nicolelis, M. A. L., and Wolf, P. D., A multichannel telemetry system for single unit neural recordings. *J. Neurosci. Methods* 133:123–135, 2004.
- Chen, H., Wu, W., and Lee, J., A WBAN-Based Real-Time Electroencephalogram Monitoring System: Design and Implementation. *J. Med. Syst.* 34(3):303–311, 2010.
- Gyselinckx, B., Penders, J., and Vullers, R., Potential and challenges of body area networks for cardiac monitoring. *J. Electrocardiol.* 40:S165–S168, 2007.
- Modarreszadeh, M., and Schmidt, R. N., Wireless, 32-channel, EEG and epilepsy monitoring system. In: 19th Int. Conf. IEEE/EMBS, IL, pp. 1157–1160. 1997.
- Farshchi, S. *et al.*, A TinyOS-enabled MICA2-based wireless neural interface. *IEEE Trans. Biomed. Eng.* 53(7):1416–1424, 2006.
- S. Farshchi, *et al.*, "Bi-Fi: An embedded sensor/system architecture for remote biological monitoring," *IEEE Trans. Inf. Technol. Biomed.*, vol. 11(6), pp. 611–618, 2007.
- R, Matthews, *et al.*, "A wearable physiological sensor suite for unobtrusive monitoring of physiological and cognitive state", 29th. IEEE EMBS Annual Int. Conf.:5276–5281, 2007.
- Emotiv EPOC. Available online: <https://emotiv.com/epoc.php>.
- Muse, the brain-sensing headband. Available online: <http://www.choosemuse.com/>. (Accessed: Dec. 2016).
- Neurosky EEG Hardware Platforms. Available online: <http://neurosky.com/biosensors/eeg-sensor/biosensors/> (Acc.: Dec2016).
- Chi, Y. M., Deiss, S. R., and Cauwenberghs, G., Non-contact low power EEG/ECG electrode for high density wearable biopotential sensor networks. In: 6th Int. Workshop on Wearable and Implantable Body Sensor Networks, pp. 246–250, 2009.
- Sullivan, T. J., Deiss, S. R., and Cauwenberghs, G., A low-noise, non-contact EEG/ECG sensor," *IEEE Biomedical Circuits and Systems Conf. (BioCAS)*, pp. 154–157, 2007.
- NXP Semiconductors. (2012). I²C-bus specification and user manual. Available: http://www.nxp.com/documents/user_manual/UM10204.pdf
- Mahajan, R., and Morshed, B. I., Performance analysis of a DRL-less AFE for battery-powered wearable EEG. *Measurement* 90: 583–591, 2016.
- R. Mahajan *et al.*, Design and Validation of a Wearable "DRL-less" EEG using a Novel Fully-Reconfigurable Architecture. 38th Annual Int. Conf. of the IEEE EMBC, pp. 4999–5002, 2016.
- Leens, F., An introduction to I²C and SPI protocols. *IEEE Instrumentation & Measurement Magazine* 12(1):8–13, 2009.

31. Hanabusa, R., Comparing JTAG, SPI, and I²C. Spansion's Application Note. pp. 1–7, 2007.
32. Myers, P., Interfacing using serial protocols: using SPI and I²C. In: Proc. ESP 2005, pp. 1–9, 2007.
33. Compumedics Lim., SynAmps RT, Detailed Overview of Functionality. <http://compumedicsneuroscan.com/synamps-rt-64-channel-eegeperp/> (Accessed: March 2016).
34. Muthukumaraswamy, S. D., High-frequency brain activity and muscle artifacts in MEG/EEG: a review and recommendations, *Frontiers in Human Neuroscience*. 7(138), 2013.
35. Ray, W. J., and Cole, H. W., EEG alpha activity reflects attentional demands, and beta activity reflects emotional and cognitive processes. *Science* 228(4700):750–752, 1985.
36. Mahajan, R., *et al.*, Reconfigurable Architecture of Neuro-Physiological Sensors for Mobile Health System. In: IEEE/ACM International Conference on Connected Health: Applications, Systems and Engineering Technologies, pp. 402–409, 2017.
37. Majmudar, C. *et al.*, Real-time hybrid ocular artifact detection and removal for single channel EEG. *IEEE Int. Conf. on Electro/Information Technology (EIT)*, IL, pp. 330–334, 2015.
38. Pacareu, S. C., Morshed, B. I., and Kozma, R., Hardware efficient seizure prediction algorithm. *SPIE Proc on Nanosensors, Biosensors, and Info-Tech Sensors and Systems*, pp. 8691:1–10, 2013.
39. Pacareu, S. C., and Morshed, B. I., Power optimization of NeuroMonitor EEG device: Hardware/Software co-designed Interrupt Driven clocking. *6th Intl. EMBS Conf. Neural Eng.* pp. 25–28, 2013.
40. BioCapture Research System, CleveMed, Available online: <https://glneurotech.com/docrepo/user-guides/BioCapture-392-0028.pdf>